Applied Energy 229 (2018) 253–263

Contents lists available at ScienceDirect

Applied Energy

journal homepage: www.elsevier.com/locate/apenergy

Flexible energy harvesting from natural gas distribution networks through line-bagging

Ermanno Lo Cascio[a], Bart De Schutter[b], Corrado Schenone[a,*]

[a] DIME - Department of Mechanical, Energy, Management and Transportation Engineering, University of Genova, via All'Opera Pia 15/A, 16145 Genova, Italy
[b] Delft Center for Systems and Control, Delft University of Technology, Mekelweg 2, Delft, The Netherlands

HIGHLIGHTS

- A novel method enabling flexible energy harvesting from natural gas distribution networks.
- Load shifting becomes possible without employing electrical storage.
- Gas bagging enables overnight charging of electric vehicles.
- Hazardous operations are avoided by employing model predictive control.
- A daily operational cost reduction of about 10% is achieved.

ARTICLE INFO

Keywords:
Energy harvesting
Natural gas
Turbo expander
Gas bagging
Electric vehicles
Night charging

ABSTRACT

In a swirling dynamic interaction, technological changes, environment and anthropological evolution are swiftly shaping the smart grid scenario. Integration is the key word in this emergent picture characterized by a low carbon footprint. Between the wide range of key actions currently pursued by European municipalities, the possibility of harvesting energy from natural gas distribution is being established in this context. Load matching is crucial for local energy exploitation and integration of renewable resources. In this paper, the authors introduce a novel management method to increase the flexibility of the energy harvesting process from gas distribution networks. This method, called gas bagging, enables one to shift energy production schedules by properly manipulating the downstream pressure of the pipeline system. The emerging system dynamics in gas bagging must be managed using a proper system control architecture. This is fundamental to avoid system-safety-constraint violations. From a relevant case scenario, the authors demonstrate that the energy load can be totally shifted to night hours without violating system-safety constraints. For this purpose, the implementation of model predictive control has revealed to be a strategic measure. In fact, this ensures safe and cost-effective operations enabling up to a 10% daily operational cost reduction. Results reveal gas bagging to be a strategic tool for energy production flexibility and carbon emission reduction using natural gas distribution networks integrated into a smart grid.

Nomenclature

D	pipeline, diameter (m)
C_{min}	heat exchanger, minimum fluid heat capacity (J/kg K)
C_{steel}	boiler, stainless steel specific heat capacity (J/kg K)
C_w	boiler, water specific heat capacity (J/kg K)
C_r	heat exchanger, heat capacity ratio
D_{Plug}	Joule-Thomson valve, plug diameter (m)
K_G	Joule-Thomson valve, flow coefficient (kg/s Pa)
c_p	hydraulic circuit, water specific heat capacity (J/kg K)
k	turbo-expander, natural gas heat specific ratio
L	pipeline, length (km)
$\dot{L}_s$	hydraulic circuit, gas preheating thermal load (W)
m	hydraulic circuit, water mass (kg)
$\dot{m}_{in}$	users, natural gas inlet mass flow rate (kg/s)
$\dot{m}_i$	header, i-th water stream mass flow rate (kg/s)
$\dot{m}_{out}$	users, natural gas outlet mass flow rate (kg/s)
$\dot{m}_w$	boiler, water mass flow rate (kg/s)

* Corresponding author.
E-mail address: corrado.schenone@unige.it (C. Schenone).

https://doi.org/10.1016/j.apenergy.2018.07.105
Received 4 May 2018; Received in revised form 10 July 2018; Accepted 22 July 2018
Available online 06 August 2018

$\dot{m}_{TE}$	turbo-expander, natural gas flow rate (kg/s)
$\dot{m}_{tot}$	user, natural gas total demand (kg/s)
M_{steel}	boiler, steel mass (kg)
M_w	boiler, water mass (kg)
P_{in}	Joule-Thomson valve, natural gas inlet pressure (Pa)
P_{out}	Joule-Thomson valve, natural gas outlet pressure (Pa)
P^*	Joule-Thomson valve, natural gas pressure at reference conditions (Pa)
P_i	pipeline, inlet pressure (Pa)
P_o	pipeline, outlet pressure (Pa)
$P_{out,TE}$	turbo-expander, outlet pressure (Pa)
q	Joule-Thomson valve, natural gas flow rate (kg/s)
$\dot{Q}_b$	boiler, thermal power output (W)
$\dot{Q}$	heat exchanger, power exchanged (W)
$\dot{Q}_{aux}$	hydraulic circuit, auxiliary heat gain (W)
R	gas constant (J/kg K)
s	Joule-Thomson valve, plug area (m^2)
T_a	hydraulic circuit, ambient temperature (K)
$T_{c,i}$	heat exchanger, cold fluid inlet temperature (K)
T_{del}	natural gas, delivery temperature at station level (K)
$T_{h,i}$	heat exchanger, hot fluid inlet temperature (K)
T_{in}	boiler, water inlet temperature (K)
T_{out}	boiler, water outlet temperature (K)
T_{out}^{header}	header, water outlet temperature (K)
$T_{out,TE}$	turbo-expander, natural gas outlet temperature (K)
T_i	header, *i*-th water stream temperature (K)
$T_{i,p}$	pipeline, average downstream temperature (K)
$T_{in,TE}$	turbo-expander, natural gas inlet temperature (K)
T_s	hydraulic-circuit water temperature (K)
T^*	Joule-Thomson valve, natural gas temperature at reference conditions (K)
T_1	Joule-Thomson valve, natural gas reference inlet temperature (K)
y	Joule-Thomson valve, actuator position (m)
W_{TE}	turbo-expander, mechanical power output (W)
V_p	pipeline, total volume (m^3)
$\dot{V}_{in}$	natural gas volumetric flow rate (m^3/h)

Greek letters

ΔT_{HE}	pre-heating heat exchanger (HE1), temperature difference (K)
ε	heat exchanger, effectiveness
κ	time instant
ρ^*	Joule-Thomson valve, natural gas density at reference conditions (kg/m^3)
η_b	boiler thermal efficiency
τ	time (s)
ρ	natural gas relative density (kg/m^3)
ζ	scaling factor

Abbreviations

BO	boiler
HE	heat exchanger
HP	high pressure
LP	low pressure
LPR	low pressure regulator
MP	medium pressure
MPC	model predictive control
NG	natural gas
TE	turbo-expander
VIGV	variable inlet guide vanes
NTU	number of transfer units
P	pump
PID	proportional, derivative, integral

1. Introduction

In the world's transition to a sustainable energy scenario, natural gas will keep playing a key role for residential and commercial sectors for most countries [1]. This issue has also been highlighted by Dieckhöner et al. in [2]. After being gathered and processed, the main phases for natural gas are transportation, storage, and distribution. Normally, the natural gas pressure is raised to 70 bars by means of compressor stations for a proper transportation through the transnational and national pipelines until the distribution nodes. At this stage, so-called pressure reduction stations are responsible for metering and reducing the gas pressure to the desired set-point for distribution purposes. Here, the natural gas pressure drop is normally induced by employing Joule-Thomson valves, thus, dissipating the gas energy. To prevent methane hydrates from being formed [3], the natural gas is normally preheated to temperatures that range between 40 °C and 60 °C depending on system operating conditions and the natural gas composition. In order to obtain a more sustainable process, a smart technological solution consists of the use of a turbo-expander (TE) instead of the Joule-Thomson valves, where the aim of the TE is to harvest energy from the gas pressure drop. In fact, Kostowski et al. analyzed the possibility of generating energy with a TE in [4] showing the engineering feasibility of such technology. Alparslan et al. presented an energy and exergy analysis of a pressure reduction station equipped with a TE in [5]. Furthermore, Borelli et al. presented a case study where a pressure reduction station is effectively integrated with other processes and users within the same district [6]. The performance analysis of the TE technology was conducted also in [7,8] where, in both cases, the energy sustainability of TE technology was demonstrated. In this case, for a given gas flow rate, the thermal energy required to prevent methane-hydrate formation would be up to 5 times higher than for the Joule-Thomson valve [9] because of the work extraction. This issue has stimulated researchers to seek for smart possibilities to reduce the carbon emissions linked to the energy-harvesting process. In fact, Kostowski et al. analyze the economic feasibility of cogeneration units in [10]. According to this study, the use of cogeneration units represents a good advantage compared with the use of boilers but low temperature heat sources might be required for gas pre-heating. In [11] an investigation of the performance of a hybrid turboexpander-fuel-cell system for power recovery at natural gas pressure reduction stations was presented. This is an interesting configuration but, economically speaking, the required initial investment might lead to a non-sustainable retrofit intervention. Other system configurations have been presented, such as in [12], where a comparative study between a pressure reduction station integrated with an internal combustion engine and an organic Rankine cycle was presented. In [13] a pressure reduction station integrated with a cogeneration system has been presented. Here, a new sizing optimization method was based on economic and thermal analysis as well. Similarly, in [14] the authors presented a novel optimization model for the optimal retrofitting of natural gas pressure reduction stations. According to this research, the use of cogeneration units tends to be economically not justifiable when the design and thus, the investment cost, is not properly defined. For this purpose, in [15], the technical criterion for economic justification of the use of cogeneration units in natural gas pressure reduction stations was presented. The authors demonstrated how only one of the eight case studies presented was suitable for cogeneration ensuring a payback period of less than eight years (which is a reasonable time length for an industrial project). Furthermore, with reference to the possibility reducing of fuel consumption for natural gas preheating by integration with renewable

resources was first analyzed by Arabkoohsar in [16], where the possibility of employing geothermal energy was examined. Furthermore, in [17] a new configuration integrated with a solar heating set was analyzed. The results demonstrated interesting opportunities deriving from solar energy integration. Similarly, in [18], the authors presented a novel configuration where the natural gas preheating is supported by parabolic trough solar collectors. According to this research, up to 33% of energy saving could be achieved in southern locations in summer periods. In [19] the possibility of integrating the pressure reduction process with 4th generation district heating networks was investigated. In [20] the control issue of a multi-carrier energy system based on a pressure reduction station was presented. In every case, the use of TE as a distributed generator has turned out to be a smart solution to enable sustainable natural gas operations. However, the energy harvesting patterns of TEs are linked to the consumption patterns of natural gas, normally characterized by diurnal peaks, thus the energy production is limited to those specific hours of the day. However, pressure reduction stations are normally located in suburban areas [20] with heterogeneous types of users. For this reason, a typical mismatch between local energy loads and TE production schedules might exist, e.g. overnight slow charging of e-buses [21].

At this stage, the use of electrical storage [22] could be an appropriate solution, but energy losses and large investment costs might lead to a non-sustainable retrofit intervention. For this purpose, in this paper, the authors introduce and analyze the possibility of employing a novel technique called gas bagging to shift the energy harvesting schedule to night hours or, in general, to a different moment. Gas bagging is based on control of the downstream distribution pressure that can be dynamically regulated as it occurs in the transportation pipeline where, the so-called gas-line-packing [23] technique is used to store the natural gas in the pipeline itself for service continuity, optimization, and speculating purposes. In addition, a set of additional advantages is hidden behind this approach. In general, the added flexibility that is generated facilitates optimal coordination with other processes or resources. For instance, gas bagging might become strategic for coordination with renewable resources, enabling optimal control in smart grids. In addition, gas bagging could unlock the service continuity issue of power-to-gas applications, enabling overnight hydrogen production for hybrid vehicles [24]. Gas bagging enables operational flexibility that could become strategic for optimal electric-vehicle charging scheduling [25] and in a market environment [26]. Furthermore, the increase of the downstream pressure leads to a proportional decrease in the process temperature i.e. the gas-preheating temperature is lower. As described in [19], the temperature reduction in pressure reduction stations is a strategic action for thermal system integration with low temperature heat sources. Thus, gas bagging can also be utilized for system thermal integration purposes. In general, gas bagging is constrained by the physical characteristics of the distribution system and safety measures, generally linked to the infrastructure location, topology and volume, pipeline geometry and type, and second-stage interconnections. Moreover, the typical pressure dynamics characterizing gas bagging should be managed by an appropriate system-control architecture in order to ensure safe operations, excluding the risk of methane-hydrate formation.

The main novelty of this paper lies in three points:

- The definition of a novel system management strategy, whose scope is to increase the flexibility of the energy harvesting process in natural gas pressure reduction stations.
- The identification of the most appropriate type of control for gas-bagging-based operations.
- The quantification of the effectiveness of gas bagging with respect to conventional operations through a case scenario analysis. Here, by conventional operations, the authors refer to those operations where the downstream pressure of the gas into the pipeline system is maintained constant during the operations.

In addition, the authors introduce a new control architecture based on a linear MPC whose scope is to maintain the TE's natural gas temperature within its limit, avoiding the formation of methane hydrates and, at the same time, ensuring higher energy performance.

This paper is organized as follows. First, the authors analyze the feasibility and the possibility of employing gas bagging to enable flexible energy harvesting in pressure reduction stations. Furthermore, an in-depth analysis of the most appropriate system control type and architecture is provided. Finally, a case study is presented. For this purpose, based on the data acquired on a plant demonstrator [18,19], a dynamic numerical model is implemented in a *Matlab-Simulink®* environment in order to analyze the system dynamics under gas-bagging-based operations for a typical configuration. Based on the system safety requirements, different types of control are analyzed in order to ensure effective gas bagging operations. These include PID controls and model predictive control (MPC) for methane-hydrate prevention. Finally, the energy and economic performance of the gas bagging are assessed for two typical scenarios in comparison with a conventional pressure reduction station, whose operations are based on constant downstream pressure. The results demonstrate the possibility of completely shifting the energy production schedule without violating any safety constraints. In conclusion, in order to assess the effectiveness of gas bagging for different downstream pipeline volumes, the system behavior has been analyzed for different pipeline lengths, respectively, 25%, 50% and 75% smaller than the initial configuration.

2. System description

In Fig. 1, a schematization of the overall system architecture is presented. For the sake of simplicity, a simplified configuration is considered in this paper but more complex systems might also be taken

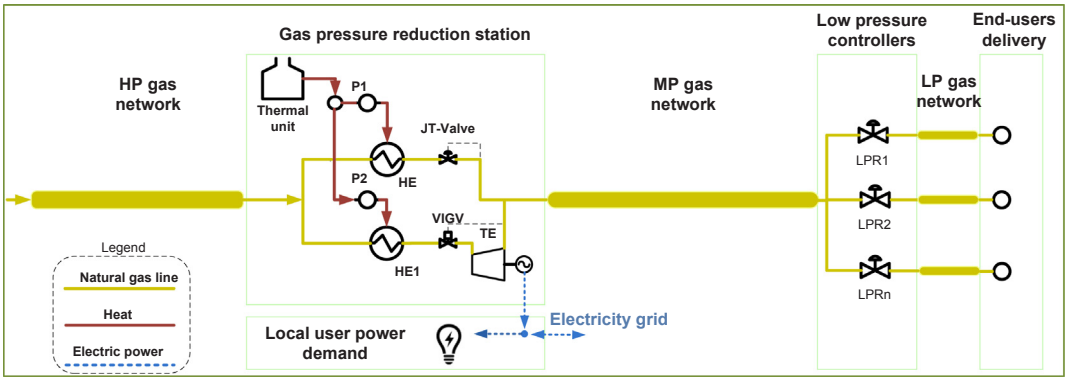

Fig. 1. Network structure and subsystem schematization.

into consideration. Indeed, the proposed system consists of a high pressure (HP) transportation pipeline, a pressure reduction station equipped with a TE working in parallel to a Joule-Thomson valve, a single straight pipe as medium pressure (MP) distribution system and, finally, a set of low pressure regulators (LPR1-3) whose scope is to bring the natural gas at lower pressure (LP) for delivery to end-users e.g. 0.5–0.04 barg. Finally, the electric output of the station can be used for local power demand e.g. to charge electric vehicles or, differently, it can be injected into the electricity grid. However, in most cases, the distribution system could be more complex than the one proposed for this research. For instance, the network topology might include nodes and interconnections that generate concentrated pressure losses enabling, for given downstream volume, a different response in the pressure transient with the respect to a straight pipeline system. In any case, it is possible to define an equivalent straight pipeline system. In addition, for a given distribution network system, there might be multiple pressure reduction stations; thus, the need of coordination between redelivery points should be properly considered during gas-bagging operations (as it is done during conventional ones). Demonstrating the effects of the interactions with other redelivery points in the presence of concentrated pressure losses is not within the scope of this research. However, the proposed simplifications have been chosen in order to use a reference system configuration, generally close to real system ones, with the final aim of demonstrating the feasibility and the performance of gas bagging.

2.1. Theoretical and technical analysis

Gas bagging is designed to increase the flexibility of energy harvesting from natural gas distribution networks. It can be performed in those pressure reduction stations equipped with TE technology. In general, gas bagging is characterized by two typical modes as described in Fig. 2: the *bagging* mode and the *un-bagging* mode. These refer to the operations performed at pressures higher and lower than the conventional set-point respectively. The maximum operating pressure during the *bagging* mode is established by the technical characteristics and safety constraints of the distribution system as will be further detailed below. The same consideration is valid for the maximum *un-bagging* pressure but, for given natural gas flow rate, pressure losses through the pipeline must be accurately considered to ensure a proper natural gas end-user delivery. In the following sections, an insight of the novel gas bagging technique is provided. Issues concerning safety and technical constraints are explored and, finally, advantages and potential applications of gas bagging are presented.

2.2. Theoretical insight

The power output of the TE depends on the inlet and outlet pressure, isentropic efficiency, and inlet mass flow rate:

$$P_{TE} = \dot{m}_{NG} c_p (T_{in} - T_{out}) \quad (1)$$

where P_{TE} and $\dot{m}_{NG}$ are respectively the TE's power output and the natural gas mass flow rate. The outlet temperature of the gas after its expansion is defined as:

$$T_{out} = T_{in}\left(\frac{P_{out}}{P_{in}}\right)^{\eta_e\left(\frac{k-1}{k}\right)} \quad (2)$$

where T_{in} and P_{in}, P_{out} and η_e are respectively the natural gas inlet temperature and pressure, the outlet pressure of the gas and the isentropic efficiency. Moreover, k is defined as:

$$k = \frac{c_p}{c_v} \quad (3)$$

where c_p and c_v are respectively the heat specific values at constant pressure and volume of the natural gas.

With reference to Eq. (2), during a gas-bagging-based operation, the TE's power output is directly linked to the dynamic pressure of the downstream distribution pipeline and, from this point, different operational issues emerge:

- A power tracking control logic is necessary for the TE's operation to achieve the desired power schedule.
- Hazardous operations might emerge due to the downstream pressure variations, leading to formation of methane hydrates. This can be prevented by implementing an MPC controller to regulate the thermal supply unit output.
- For a given time length, the energy production of the gas bagging should be equivalent to that of the conventional mode in order to avoid energy losses.

2.3. Technical feasibility and bounds

The topology and dimension of the distribution system determine the possibility of performing gas bagging and its degree of flexibility, i.e. maximum and minimum bagging pressure. More precisely, pipelines can be categorized according to their pressure bounds [27], as shown in Table 1. Normally, for distribution, natural gas is delivered at pressures up to 24 barg to pressure reduction stations [28], but higher redelivery pressures could be adopted. Downstream, the distribution system is characterized by steel or polyethylene pipes whose design characteristics and installation criteria are strictly regulated by national standards as described e.g. in [27]. In general, distribution pipe diameters range from 5 to 50 cm and, the network topology, gas flows, and operating pressures are intimately linked to the territory characteristics; these are quite diverse from place to place. In fact, some operators manage up to 44 km of pipelines at medium pressure [29], while others manage about 141 km of medium pressure pipeline [30] or 127 km of pipeline of 4th category [31]. Thus, the degree of flexibility of the gas bagging might change considerably from case to case. Furthermore, before adopting gas bagging, the calibration of the so-called monitor valve, the one placed upstream of the Joule-Thomson valve, should be re-done considering the pressure variations that occur during gas

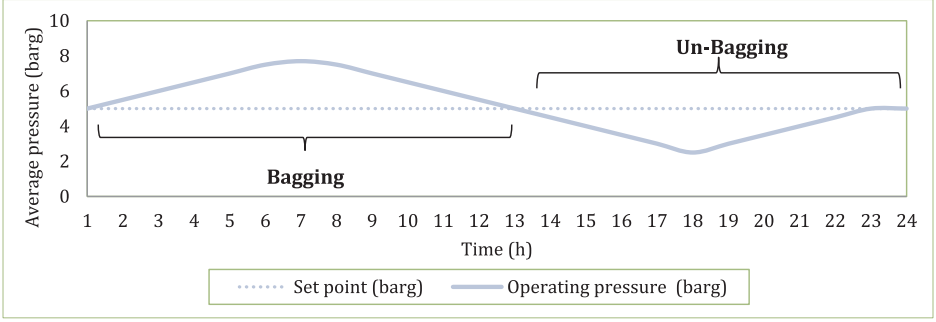

Fig. 2. Gas bagging mode representation.

Table 1
Categorization of pipeline [27].

Category	1st	2nd	3rd	4th	5th	6th	7th
Minimum pressure (bar_g)	24	12	5	1.5	0.5	0.04	–
Maximum pressure (bar_g)	–	24	12	5	1.5	0.5	0.04

bagging. The same precautions must be adopted for all the pressure reduction stations connected to the gas distribution infrastructure. Furthermore, the *un-bagging* mode must be properly constrained considering gas pressure losses through pipelines during gas demand peaks. Finally, for given inlet gas pressure, the gas-bagging operation will be constrained by the maximum mass flow rate of the TE and by the maximum power output of the permanent magnet synchronous generator driven by the TE's shaft.

2.4. Regulatory and safety constraints

In the current state, national regulations for gas distribution are characterized by similar constraints spontaneously determined by safety issues. These are mainly related to the relief pressure set point of the distribution system that, e.g. for the Italian case [27] must be less than or equal to 115% of the maximum admissible pressure of the pipeline. Other constraints are related to the pipeline sections close to buildings and roads. In these cases, some restrictions on the operating pressure might be foreseen, thus considerably limiting the flexibility of the gas bagging. At this stage, it is worth recalling that these regulations could be less constraining for future infrastructure mainly due to technological changes and material improvements. Finally, qualitatively speaking, the overall frequency of gas leaks should be equivalent to those related to the conventional operation since, *bagging* mode gas leaks should be balanced by those of the *un-bagging* mode.

2.5. Control for gas bagging

In standard configurations, natural gas pressure reduction stations are equipped with two redundant gas-fired-boiler units. These are necessary to provide the required heat for the process in order to prevent formation of methane hydrates which depends on the natural gas composition and the operating conditions. The local control logic of the boilers is normally characterized by a constant operating set-point that is manually adjusted by the plant's operators based on the season [19]. However, in gas-bagging-based operations, the necessity to employ a higher-level control to optimize process temperature emerges for safety and energy reasons. In fact, the pressure dynamics activated are faster than the thermal response of the heat supply system due to thermal inertia. For this reason, in certain situations and for a given temperature set-point, decreases in the downstream pressure could drag the system into hazardous operations achieving hydrate formation temperature at the outlet of the TE. This is because the heat supply response might not be fast enough in conventional control. A solution to this problem could be given by the use of a higher water-temperature set-point: however, this action would lead to inefficient operations thereby increasing carbon emissions. Thus, PID control and MPC are appropriate tools to adopt, for safe operations and fuel-consumption optimization. MPC can be used to control a great variety of processes, from those with relatively simple dynamic to more complex ones, including systems with long delay time or non-minimum phase or unstable ones [32]. The TE's power output and the downstream pressure are the process variables to be scheduled or dynamically controlled during gas bagging. The TE's schedule could be optimized itself enabling even lower carbon emissions.

3. Reference system modeling

In this section, the authors propose an in-depth transient analysis based on the system configuration of Fig. 1. For this purpose, a numerical model has been implemented in a *Matlab-Simulink®* environment. For this kind of system, the key parameters that play a key role in methane-hydrate formation are the thermal inertias of the water contained in the hydraulic circuit and the metal mass of the boiler. This requires the modeling approach to be fully dynamic in order to achieve accurate results. This allow the authors to model other components with a steady state approach while dealing with dynamic conditions. The numerical model validation was based on data acquired during real plant monitoring [19] basing on a demonstrator located in the city of Genoa (Italy). Two typical case scenarios are considered that are related to summer and winter operations. Furthermore, an energy and economic comparison between conventional and gas-bagging operations is performed for different control architectures respectively based on a constant temperature set-point for the boiler control unit, PID control and MPC. In Fig. 3a–c, a schematization of each control architecture adopted is represented, while in Table 2 the control parameters are reported.

3.1. Thermal unit

The energy model of the boiler unit [33] is given by Eq. (4):

$$C_{tot}\frac{dT_{out}}{d\tau} + \dot{m}_w c_{p,w}(T_{out} - T_{in}) = \dot{Q}_b \tag{4}$$

in which C_{tot} was determined by:

$$C_{tot} = M_{steel}C_{steel} + M_w C_w \tag{5}$$

where $\dot{Q}_b$ is the boiler output while M_{steel}, C_{steel}, M_w and C_w stand for the boiler metal mass, stainless-steel heat capacity, water mass, and water heat capacity respectively.

3.2. Heat exchangers

A steady-state approach is used to model the heat exchanger units. This is because the thermal inertia of the metal mass and water can be considered negligible compared with the thermal inertia of the

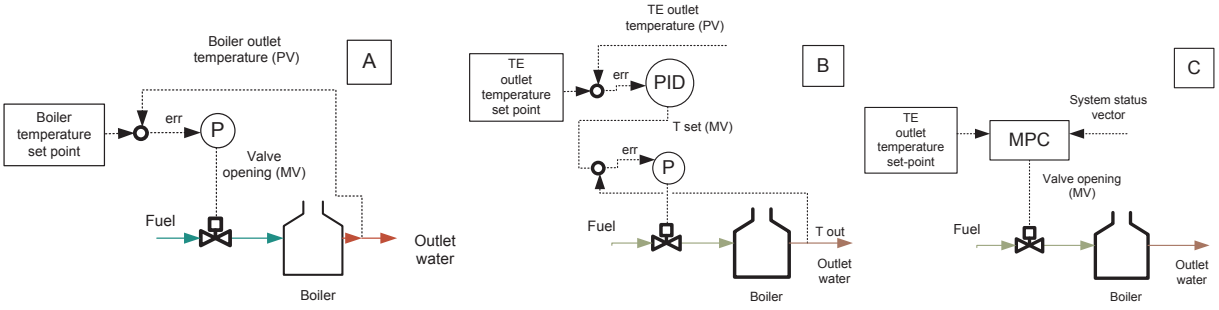

Fig. 3. Control architecture: (a) Constant temperature; (b) PID Optimization; (c) MPC optimization.

Table 2
Control parameters.

Control type	Value
Constant temperature, set point (K)	360
PID optimized set point, P;I;D (K)	10;1;0

hydraulic circuit. This is based on the effectiveness-NTU (number of transfer units) method [34]. All the heat exchangers were modeled with the counter-current flow configuration to increase effectiveness. The effectiveness (ε) and the number of transfer units (NTU) are determined by:

$$\varepsilon = \frac{1-e^{[-NTU(1-C_r)]}}{1-C_r e^{[-NTU(1-C_r)]}} \tag{6}$$

$$NTU = \frac{UA}{C_{min}} \tag{7}$$

where UA is the overall heat transfer coefficient and C_r is the ratio between the minimum and the maximum heat capacity of the two fluids.

The heat exchange between the two fluids is defined by:

$$\dot{Q} = \varepsilon C_{min}(T_{h,i}-T_{c,i}) \tag{8}$$

where $T_{h,i}$ and $T_{c,i}$ are the hot and cold fluid inlet temperatures, respectively.

3.3. Hydraulic circuit

The thermal inertia effects on the system dynamic are modeled by considering an equivalent water tank model. This component is implemented based on [35]. For simplicity, the temperature gradient was considered to be heterogeneously distributed in the control volume. Thus, the energy balance is given by:

$$(mc_p)\frac{dT_s}{d\tau} = \dot{Q}_{aux}-\dot{L}_s-(UA)(T_s-T_a) \tag{9}$$

where m and c_p are the water mass contained in the tank and its specific heat value; T_s and T_a stand for water and ambient temperatures, respectively; $\dot{L}_s$ represents the thermal power required by the preheating process and $\dot{Q}_{aux}$ is the auxiliary boiler thermal gain.

3.4. Joule-Thomson valve

In natural gas pressure reduction stations, control of Joule-Thomson valves is purely pneumatic. Thus, the downstream and upstream gas pressure act on a diaphragm whose scope is to regulate the desired actuator position. The set-point is regulated by operators intervening on a balancing spring. In a gas-bagging-based operation, retrofit measures on the valve control have to be undertaken. These consist of the implementation of a remote-controllable actuator whose scope is to follow the opening schedule for gas bagging. For simulation purposes, the actuator opening was managed by a PID controller in the conventional operation simulation and by a pre-designed schedule for the gas-bagging-based operations. The modeling approach used in [36] are also implemented in this study. The temperature variations caused by the Joule-Thomson effect are modeled by considering a coefficient of 4.778 K/MPa [37]. The natural gas mass flow passing through the valve (q) is defined as:

$$q = K_G\sqrt{P_{in}(P_{in}-P_{out})} \tag{10}$$

in which the flow coefficient of Joule-Thomson valve (K_G) was determined by:

$$K_G = s\sqrt{2\frac{\rho^* T^*}{P^* T_1}} \tag{11}$$

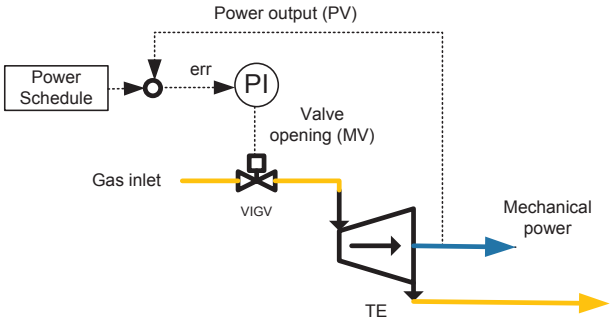

Fig. 4. TE control architecture.

where s denotes the flow area at the plug; P^*, T^*, ρ^*, respectively stand for pressure, temperature and density at the reference conditions. The plug area s depends on the actuator position (y) and the plug diameter (D_{plug}):

$$s = yD_{Plug} \tag{12}$$

3.5. Turbo expander

Normally, every TE has its own performance map where the mass flow rate passing through the machine with respect to the pressure ratio and the isentropic efficiency are reported. In addition, in Fig. 4, the control architecture of the TE is presented. However, the TE was implemented by considering Eqs. (1)–(3) and the variable inlet guide vanes (VIGV) of the TE, used to control the mass flow rate, were modeled by using valve model i.e. Eqs. (10)–(12). In addition, during a gas-bagging operation, the pressure transients would affect the mass flow entering the TE thus influencing the power production. So, in order to keep the power production stable, a proportional and integral controller has been implemented in the gas-bagging model as shown in Fig. 3. Here, the process variable (PV) is the mechanical power output of the TE while the manipulated variable (MV) is the valve opening (y). The proportional and integral values were respectively 0.001 and 0.0005 m.

3.6. Header

The outer temperature of the header component, denoted by T_{out}^{header}, where the diverse flows converge, is modeled as follows:

$$T_{out}^{header} = \sum_i \frac{\dot{m}_i T_i}{\dot{m}_i} \tag{13}$$

where $\dot{m}_i$ and T_i are the mass flow rate and the temperature of the i-th water stream, respectively.

3.7. Distribution pipeline

Normally, to model the pressure dynamics in pipeline systems, isothermal or non-isothermal models derived from energy, momentum, and mass balance equations are used [38]. The solution method of partial differential equations is normally based on a finite-differences method. In this study, to achieve faster simulations, the authors employ an isothermal lossless modeling approach to estimate pressure variations at the inlet of the straight pipeline [39]. The choice of an isothermal model is suitable due to the slow pressure dynamics involved. In addition, the limited pipeline length makes the use of a lossless model favorable ensuring realistic results. More precisely, the pressure dynamics at the inlet of the pipeline segment were modeled by:

$$\frac{dP_i}{d\tau} = \frac{RT_i}{V_p}(\dot{m}_{in}-\dot{m}_{out}) \tag{14}$$

where P_i, R, T_i, V_p, $\dot{m}_{in}$, $\dot{m}_{out}$ respectively stand for the natural gas pressure at the inlet of the pipeline segment, the gas constant, the inlet temperature and the volume of pipeline, the inlet, and the outlet gas mass flow rate of the pipe segment.

The downstream pressure at the end of the straight pipe is modeled by using Renouard's model [40], which is used for designing networks:

$$P_i^2 - P_o^2 = (46742)\rho L \dot{V}_{in}^{1.82} D^{-4.82} \quad (15)$$

where P_i and P_o represents the pipeline inlet and outlet pressure respectively, ρ stands for the gas relative density, and L, $\dot{V}_{in}$ and D are the pipeline length, gas volumetric flow, and diameter of the pipe section.

3.8. Model predictive control implementation

The BO unit control was implemented using linearized MPC. This enabled fast simulations without affecting system performance. In fact, no constraint violations were detected during plant simulations. The MPC implementation was made with a Level 2 S-Function [41] in *Matlab-Simulink®*. This allows users to define a custom block through *Matlab* script and to set the desired block time sampling for the simulation (120 s). Several processes using variables were measured. These were utilized to compute the optimization process using the interior-point optimization algorithm of the fmincon solver of the *Matlab* toolbox. Furthermore, the manipulated variable i.e. the fuel mass flow rate that feeds the boiler, is sequentially updated. The measured variables of the process at time κ were the natural gas flow rate $\dot{m}_{TE}^{\kappa}$, the TE's outlet and inlet temperature of the natural gas $T_{in,TE}^{\kappa}$ and $T_{out,TE}^{\kappa}$, the boiler thermal efficiency η_B^{κ}, the delivery temperature of the natural gas T_{del}^{κ}, the TE's inlet pressure P_{in}^{κ} and the isentropic efficiency η_e^{κ}. To estimate the temperature of the natural gas at the TE's outlet at time $\kappa + 1$, the following model was employed:

$$T_{out,TE}^{\kappa+1} = T_{out,TE}^{\kappa} + \zeta[T_{out,TE}^{\kappa} - \beta^{\kappa}(T_{del}^{\kappa} + \Delta T_B)] \quad (16)$$

where ζ is a dimensionless scaling factor whose value has been heuristically optimized in order to achieve a stable control behavior by means of several tests and β^{κ} is defined as:

$$\beta^{\kappa} = \left(\frac{P_{out}^{\kappa}}{P_{in}^{\kappa}}\right)^{\eta_e^{\kappa}\left(\frac{k-1}{k}\right)} \quad (17)$$

In Eq. (16) ΔT_B represents the water temperature difference that occurs in the boiler unit. This is derived from an energy balance in the boiler unit:

$$\eta_B^{\kappa} \dot{m}_{fuel} LHV = \dot{m}_w^{\kappa} c_p \Delta T_B \quad (18)$$

For the sake simplicity, the pre-heating of the natural gas is assumed to occur with no energy loss:

$$\eta_B^{\kappa} \dot{m}_{fuel} LHV = \dot{m}_{TE}^{\kappa} c_{p,gas} \Delta T_{HE} \quad (19)$$

where ΔT_{HE} is the temperature increase that occurs in the natural gas preheating heat exchanger (HE1). Finally, by substituting Eqs. (17) and (18) in Eq. (16), Eq. (20) represents the natural gas at the outlet temperature of the TE at time step $\kappa + 1$:

$$T_{out,TE}^{\kappa+1} = T_{out,TE}^{\kappa} + \zeta\left\{T_{out,TE}^{\kappa} - \beta^{\kappa}\left[T_{del}^{\kappa} + \left(\frac{\eta_B^{\kappa}\dot{m}_{fuel} LHV}{\dot{m}_{TE}^{\kappa} c_{p,gas}}\right)\right]\right\} \quad (20)$$

From Eq. (16), the optimization problem formulation is:

$$\min \dot{m}_{fuel}(T_{out,TE}^{\kappa}, T_{out,TE}^{\kappa+1}, \zeta, T_{out,TE}^{\kappa}, \beta^{\kappa}, T_{del}^{\kappa}, \eta_B^{\kappa}, LHV, \dot{m}_{TE}^{\kappa}, c_{p,gas}) \quad (21)$$

subject to:

$$275 - T_{out,TE}^{\kappa} \leqslant 0 \quad (22)$$

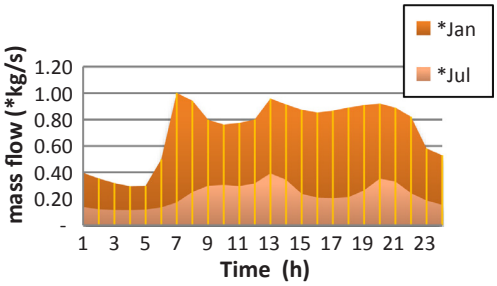

Fig. 5. Natural gas (*normalized flows).

4. Results and discussion

In this section, the results relative to two relevant case scenarios are reported.

4.1. Simulation scenarios

The relevant case scenarios considered in this study are linked to typical flow patterns for a natural gas distribution system located in Italy [18]. As shown in Fig. 5, the authors considered July and January flow patterns for gas-bagging proof of concept purposes. This is because the most hazardous operations could normally emerge during these periods, where the natural gas flows are at their respective bounds. Furthermore, for each scenario, two sets of simulations were performed: one related to the conventional operation where the TE's power output is driven by the natural gas flow rate and the equivalent simulations for the gas-bagging-based operation. The latter were carried out by imposing a power production schedule on the TE and on the Joule-Thomson valve. To maintain the TE's power production schedule during downstream pressure transients, a PID controller was used. This, acting on the VIGV of the TE, enables proper power production. For each set of simulations, different control architectures were considered for the thermal unit outlet temperature: constant set-point, PID optimized set-point, and linearized MPC. Finally, in order to assess the effectiveness of gas bagging, for a daily time frame, the same energy production was imposed in the conventional simulations. In Table 3, the component design characteristics are reported, while in Table 4, the simulation initial conditions, which were kept equal in both the conventional and gas-bagging simulations, are detailed.

4.2. Winter functioning

Thus, for the conventional winter case (Fig. 6a–d), in 24-h operation, the total energy harvesting is about 12 MW h. As shown in Fig. 6d, the energy production is concentrated in diurnal hours due to the typical patterns that characterize natural gas distribution. As shown in Fig. 6a, the TE reaches its maximum power output for most of the day. The delivery pressure considerably decreases to a minimum of about 1 barg while the MPC controller does not lead to constraint violations for the TE's outlet temperature, i.e. the risk of methane hydrates can be excluded (Fig. 6b–d). The same energy output, can be shifted to night hours with the gas bagging (Fig. 6e–h). In this case, a maximum bagging pressure of about 8 barg is achieved. Following Fig. 6d, in order to compensate the downstream-pressure increase, the TE's PID controller gradually increases the gas flow rate during the *bagging* mode without overstepping the maximum inlet gas mass flow rate of the TE. The minimum pressure achieved (Fig. 6f) in the gas *un-bagging* mode is about 0.75 barg. This is enough to guarantee a proper operation for the low-pressure regulators. However, the risk of achieving too low delivery pressures can be attenuated by opening the Joule-Thomson valve, enabling pressure increase. Finally, the gas temperature at the outlet of the TE remains close to the set-point thanks to the MPC controller, i.e. the risk of formation of methane hydrates is avoided.

Table 3
Component details.

Component	Value	Component	Value
Number of JT lines [–]	1	TE, power tracking PI gains (gas bagging)	1e−4; 5e−5
HE overall UA [kW/K]	1.5	BO, nominal power [kW]	1500
HE1, overall UA [kW/K]	16	BO, steel and water mass [kg]	1998; 950
TE, model, *Honeywell*	*MTG550*	BO, steel [kJ/kg K]	502
TE, nominal mechanical power [kW]	550	BO, fuel, P gain (conventional) [kg/s]	9e−4
TE, VIGV, PI gains (conventional) [m]	3.16e−5; 2.71e−8	Hydraulic circuit volume [m^3]	17.6
TE, set point (conventional) [bar]	5.1	Hydraulic circuit heat transfer area [m^2]	25.9
JT-Valve set point (conventional) [bar]	5	Hydraulic circuit overall UA [W/K]	10.4
JT-Valve plug diameter D_{plug} [cm]	5	Downstream pipe diameter [mm]	50
P1, P2, mass flow rate [kg/s]	8; 11.1	Downstream pipe length [km]	118

Table 4
Initial conditions of the simulations.

Component	Value	Component	Value
boiler outlet temperature (K)	360.15	HP pipeline redelivery pressure (barg)	25
MP pipeline inlet pressure (barg)	5	hydraulic circuit temperature (K)	360.15

4.3. Summer functioning

In Fig. 7a–d, it is possible to observe the dynamic behavior of the system for the conventional operation in a typical summer scenario. More precisely, the total TE energy production is about 5 MW h per day. The minimum gas delivery pressure at the end of the pipeline segment is relatively high due to the lower mass flow with respect to the winter case. No hazardous operations are detected in this case. Furthermore, in Fig. 7e–h, the dynamic behavior of the system for the bagging operation is presented. Here, a maximum bagging pressure of about 9 barg is achieved, while the modest gas flow rate involved does not seem to significantly affect the delivery pressure at the end of the pipeline. Finally, no violation of the TE's outlet gas temperature was observed thanks to predictive control.

4.4. Pipeline length reduction

In this section, the gas-bagging effectiveness is analyzed for different pipeline lengths. More precisely, the system behavior has been analyzed for a pipeline length of about 88.125 km (75% smaller), 58.750 (50% smaller) and finally for 29.375 km (75% smaller). For this purpose, the power schedule of the TE has been kept the same during the simulation while, the valve opening has been adjusted in order to satisfy the system pressure constraints (13.8 bars) [27]. In Fig. 8a–d, the system behavior for a pipeline length reduction of about 25%. In this case, no pressure constraint violations are detected. In addition, the MPC's response is fast enough excluding any risk of methane-hydrate formation. Instead, for the 50%case (Fig. 8e-h) the pressure achieves a maximum value of about 14 barg, which is slightly higher than the maximum admissible pressure foreseen by Italian standards. The case with a 75% reduction of the pipeline length (8i-n), is infeasible since the operating conditions are considerably higher than their maximum. In this case, the only way to proceed with gas bagging, is to redefine the power schedule in order to reduce the overall daily energy production. Practically speaking, the TE's power production should be limited to smaller quantities.

In Table 5 the results of gas bagging are presented. Here it is possible to observe how a length reduction of 25% does not compromise the energy production schedule with energy penalization; thus the amount of energy that is lost due to the pressure dynamics, is equal to 0. Differently, if the initial length is 50% smaller, a 25.8% energy loss is recorded with respect to the initial case (12 MW h). This is because the downstream pressure is relatively too high; thus limiting the specific work output of the TE. This aspect is further highlighted in the case in which the pipeline length is 75% lower than the initial case. More precisely, this scenario would be infeasible since the TE should operate over its admissible operating conditions. In addition, the maximum

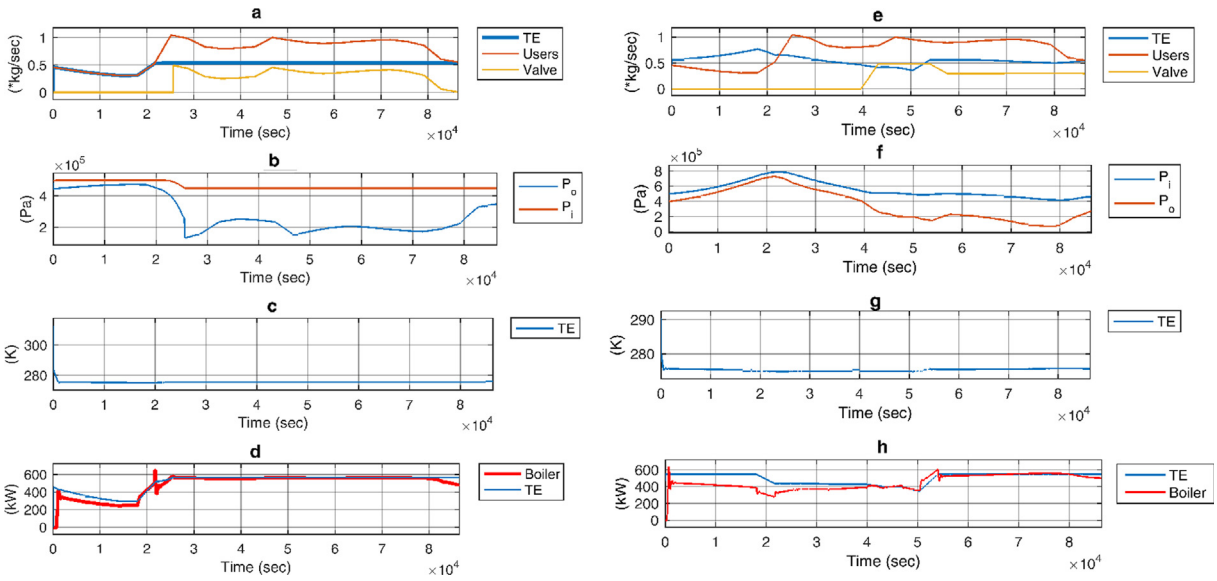

Fig. 6. Winter scenario: (a–d) Conventional; (e–h) gas bagging.

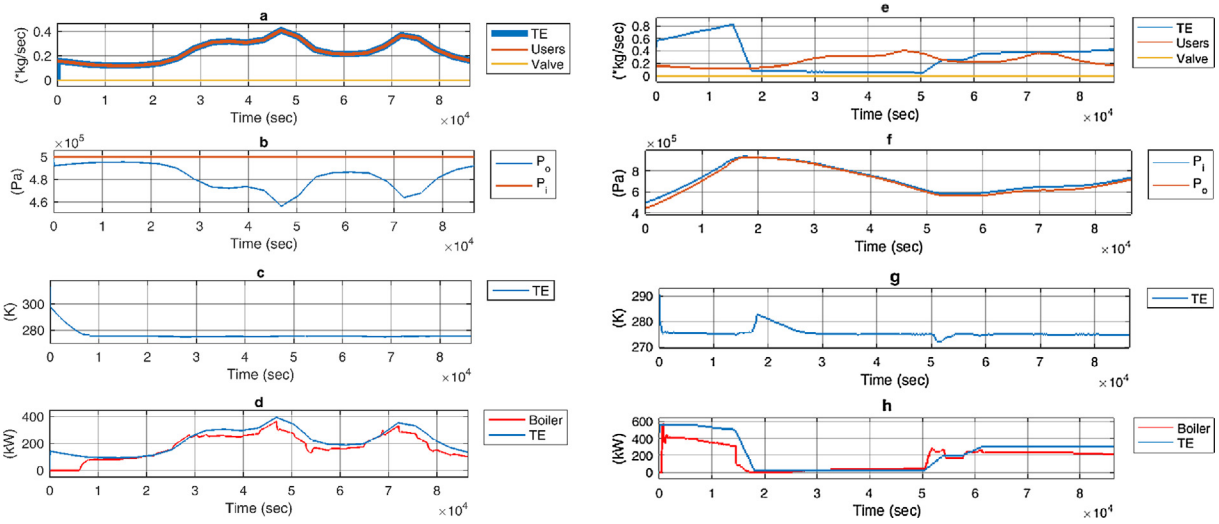

Fig. 7. Summer scenario: (a–d) Conventional; (e–h) gas bagging.

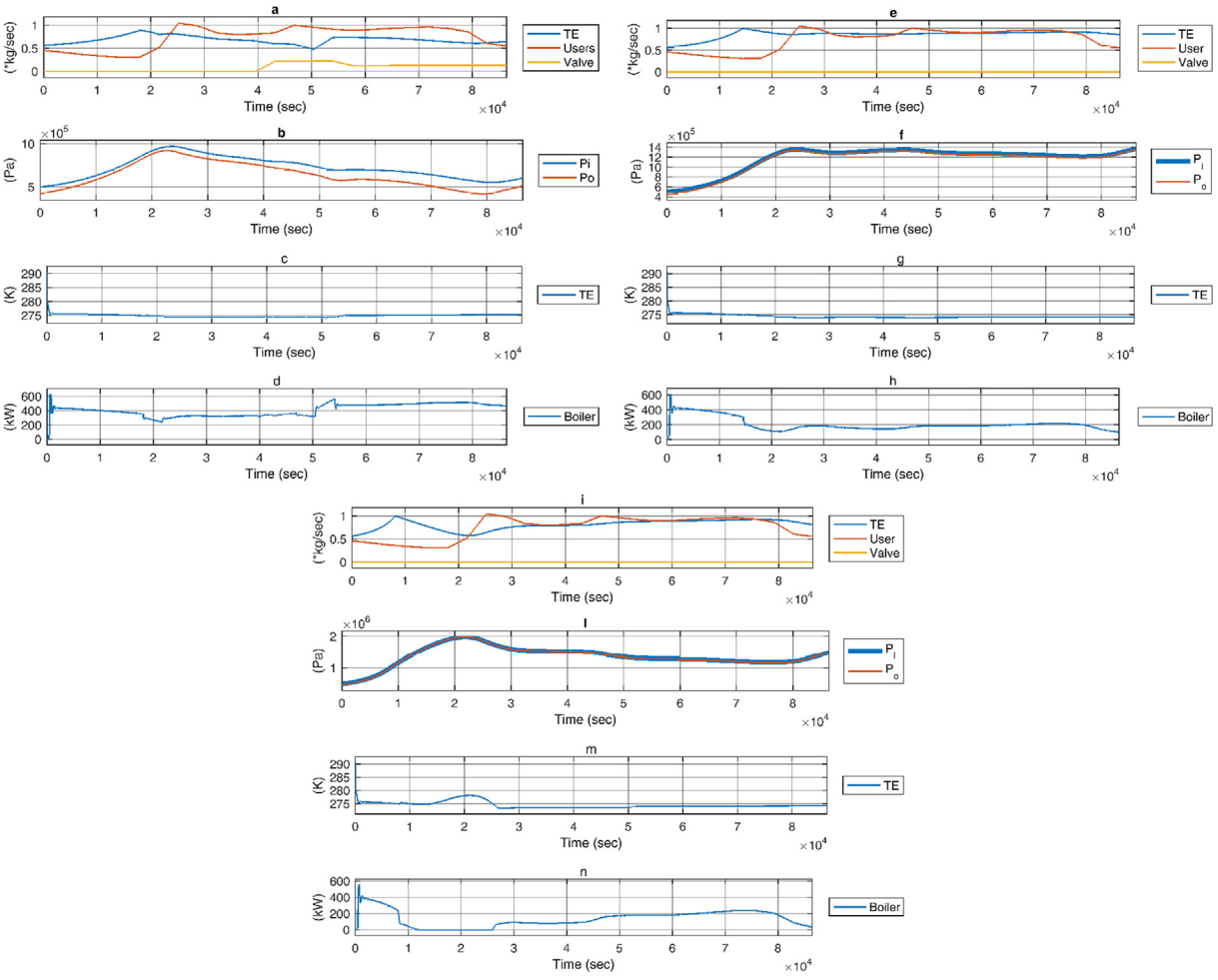

Fig. 8. Reduced pipeline length. (a–d) 25%; (e–h) 50%; (i–n) 75%.

Table 5
Gas-bagging assessment.

Case	Pipeline length (km)	Energy penalization (%)	Scenario
25% reduction	88,125	0	Feasible
50% reduction	58,750	25.8	Feasible
75% reduction	29,375	41.6	Unfeasible

bagging pressure achieved in this case would be higher than 15 barg, while the admissible pressure for the pipeline category is 13.8 barg.

4.5. Discussion and recommendations

In Table 6, the operational performance of the system for the gas-bagging mode are reported in comparison to the conventional mode for

Table 6
Gas bagging versus conventional:

Case	Mode	Control	Fuel cost (euro)	Gross income (euro)	TE output P (kWh)	Average TE isentropic efficiency	Thermal unit energy output Q (kWh)	Average thermal efficiency	Boiler behavior	P/Q (–)	Average outlet temp. (K)	Operation
January	Gas Bagging	Constant T	816	505.10	12,010	0.54	11,050	0.73	No Oscillations	1.09	278	Hazardous
		PID	800	521.10	12,010	0.54	10,825	0.73	Oscillations	1.11	277	Hazardous
		Linear MPC	800	520.00	12,000	0.54	10,800	0.73	No Oscillations	1.11	275	Safe
	Conventional	Constant T	850	470.00	12,000	0.54	11,640	0.75	No Oscillations	1.03	278	Safe
		PID	767	564.00	12,100	0.54	10,330	0.73	Oscillations	1.17	271	Hazardous
		Linear MPC	848	437.90	12,100	0.54	11,690	0.74	No Oscillations	1.04	275	Safe
July	Gas Bagging	Constant T	430	157.95	5345	0.48	5320	0.65	No Oscillations	1.00	298	Safe
		PID	387	200.95	5345	0.48	4763	0.63	No Oscillations	1.12	289	Safe
		Linear MPC	330	256.30	5330	0.45	4000	0.62	No Oscillations	1.33	275	Safe
	Conventional	Constant T	414	175.82	5362	0.50	4893	0.64	No Oscillations	1.10	282	Safe
		PID	377	210.62	5342	0.52	4700	0.63	Oscillations	1.14	280	Safe
		Linear MPC	365	218.00	5300	0.50	4320	0.63	No Oscillations	1.23	276	Safe

the winter and the summer case scenarios. For each of them, three different control architectures have been tested for the thermal unit control. Namely, constant temperature, PID, and MPC. Following, the fuel cost, calculated as the fuel mass consumed multiplied by a reference constant price (€0.8/kg) is reported together with the gross income calculated as the difference between the income generated by the electricity production (€0.15/kWh) minus the operational cost. In addition, the value of the average isentropic efficiency of the TE and the average boiler thermal efficiency are shown in Table 6. These are calculated as the integral over the 24-h operations. Furthermore, with reference to the thermal unit control, the possibility of observing unstable behavior of the controller might arise. This is specially verified when employing PID controller. To address this issue, the authors have defined a qualitative index named *boiler behavior* as reported in Table 6. When oscillation occurs, frequent step changes, ranging from the lower to the upper bound were, observed. This behavior might be difficult to avoid even with a proper tuning of parameters. Thus, being not physically acceptable, this kind of behavior must be avoided. Furthermore, the average outlet temperature of the gas is reported in Table 6. This is calculated as the integral over the 24 h operation. Finally, in the last column of Table 6, the risk of methane-hydrate formation is presented. A hazardous operation occurs when the natural gas temperature leaving the TE goes below 2 °C during system operations. Differently, the operation can be considered safe. In addition, for the given case scenario, the application of gas bagging to those systems with smaller downstream distribution system is possible for pipeline networks longer than 88.125 km (0.5 m in diameter) with an energy penalization of about 25.8%. For smaller distribution networks, it is highly recommended to limit the power production schedule in order to reduce the daily energy production.

Finally, for the case study presented, it was possible to perform the gas-bagging operation and the MPC control architecture turned out to be the most appropriate option which guaranteed cost-effective system operations for this case study. Gas-bagging operations result to be more economically convenient with respect to the conventional mode. This is due to the complex system dynamics involved which, in general, foresee different operations of the TE and the Joule-Thomson valve. At this stage, it is worth recalling that it might be possible to determine the optimized operating schedule, i.e. optimal bagging and un-bagging pressure, which could lead to even better performing operations.

With reference to Table 6, for the gas-bagging simulations, for the winter case scenario, a modest decrease in the operational costs can be observed for the conventional mode for constant set-point, PID, and MPC-based thermal unit control respectively. This issue is linked to the Joule-Thomson valve opening which occurs with different dynamics between the two modes. In any case, MPC ensures a safe operation in both simulation scenarios. Moreover, MPC enables a stable behavior of the thermal units compared to PID control, which tends to generate undesired thermal load oscillations. With reference to the gas-bagging summer scenario of Table 6 instead, MPC is capable of significantly reducing the operational cost by 23.3% per day with respect to the constant temperature control, while ensuring safe operating conditions. This operational cost reduction is more emphasized during summer than winter since, for a given temperature set-point for the control of the boiler unit, at lower gas mass flow rate, a thermal overproduction occurs. This means that the natural gas is excessively preheated before entering the TE. As a result, the outgoing natural gas will be uselessly, relatively hot. Thus, an optimized control has shown that it enables significant energy saving.

5. Conclusions

In this paper, the authors have presented a novel system management strategy to harvest energy from natural gas distribution networks. This method, called gas bagging, enables flexible system operations in the so-called natural gas pressure reduction stations equipped with turbo-expander technology. In fact, by appropriately managing the downstream pressure of the gas, the energy production can be shifted to a desired moment. The degree of flexibility of gas bagging is strongly dependent on the technical characteristics and the safety constraints of the pipeline system. The risk of conducting hazardous operations can be properly managed by employing a model predictive controller for the boiler units. In addition, a model predictive controller enables operational cost reduction. Thus, from a reference case scenario consisting of a pipeline of 118 km, the authors have demonstrated through numerical dynamic simulations that gas bagging allows to completely shift the energy production to night hours while maintaining safe operations. Furthermore, the results highlighted that, for the proposed case study, a daily decrease of about 6% of the operational cost in the winter operations can be achieved with gas bagging. Similarly, in summer periods, the operational cost reduction was about 10%. In addition, for given power production schedule, the effectiveness of gas bagging for pipeline lengths smaller than 25%, 50%, and 75% was assessed. Results demonstrated that the 25% reduction did not affect the gas-bagging effectiveness or the energy production. At the same time, gas bagging can be performed safely without any system-constraint violation. This condition is verified by reducing the pipeline length by 50%. In this case, the system operates at its maximum tolerable conditions and an energy loss of about 25.8% has been recorded with respect to the initial case scenario (117 km of pipeline). For smaller distribution volumes, in order to perform gas bagging, the power production schedule must be limited in order to reduce the energy production. Finally, gas bagging can be performed at different pressure levels and for different volumes of the pipeline system, but accurate analysis and tests must be conducted before implementation in order to ensure safe operations. Concluding, gas bagging has revealed itself to be a strategic method to

increase energy harvesting flexibility from natural gas distribution networks enabling better integration into smart grids contexts. Future research steps should involve an in-depth analysis of the environmental performance of the gas bagging compared with the conventional operations. Further, simulations using computational fluid dynamics for an in-depth understanding of downstream distribution phenomena under variable boundary conditions and optimal scheduling should be consider as well.

References

[1] W. E. Outlook. http://www.worldenergyoutlook.org/publications/weo-2016/; 2016 [accessed 21.03.18].
[2] Dieckhöner C, Lochner S, Lindenberger D. European natural gas infrastructure: the impact of market developments on gas flows and physical market integration. Appl Energy 2013;102:994–1003.
[3] Chen J, Liu J, Chen G, Sun C, Jia M, Liu B, et al. Insights into methane hydrate formation, agglomeration, and dissociation in water + diesel oil dispersed system. Energy Convers Manage 2014;86:886–91.
[4] Kostowski W. Possibility of energy generation within the conventional natural gas transport system. Strojarstvo: časopis za teoriju i praksu u strojarstvu 2010;52(4):429–40.
[5] Alparslan M, Ozgener O, Ozgener L. Energy and exergy analysis of electricity generation from natural gas pressure reducing stations. Energy Convers Manage 2015;93:109–20.
[6] Borelli D, Devia F, Lo Cascio E, Schenone C, Spoladore A. Combined production and conversion of energy in an urban integrated system. Energies 2016;9:1–17.
[7] Andrei I, Valentin T, Cristina T, Niculae T. Recovery of wasted mechanical energy from the reduction of natural gas pressure. Procedia Eng 2014;69:986–90.
[8] Xiong Y, An S, Xu P, Ding Y, Li C, Zhang Q, et al. A novel expander-depending natural gas pressure regulation configuration: performance analysis. Appl Energy 2018;220:21–35.
[9] Lo Cascio E, Borelli D, Devia F, Schenone C. Key performance indicators for integrated natural gas pressure reduction stations with energy recovery. Energy Convers Manage 2018;164:219–29.
[10] Kostowski WJ, Usón S. Thermoeconomic assessment of a natural gas expansion system integrated with a co-generation unit. Appl Energy 2013;101:58–66.
[11] Howard C, Oosthuizen P, Peppley B. An investigation of the performance of a hybrid turboexpander-fuel cell system for power recovery at natural gas pressure reduction stations. Appl Therm Eng 2011;31:2165–70.
[12] Kostowski WJ, Usòn S. Comparative evaluation of a natural gas expansion plant integrated with an IC engine and an organic Rankine cycle. Energy Convers Manage 2013;75:509–16.
[13] Sanaye S, Nasab AM. Modeling and optimizing a CHP system for natural gas pressure reduction plant. Energy 2012;40:358–69.
[14] Lo Cascio E, Puig Von Friesen M, Schenone C. Optimal retrofitting of natural gas pressure reduction stations for energy recovery. Energy 2018;153:387–99.
[15] Farzaneh-kord V, Khoshnevis AB, Arabkoohsar A, Deymi-dashtebayaz M. Defining a technical criterion for economic justification of employing CHP technology in city gate stations. Energy 2016;111:389–401.
[16] Farzaneh-gord M, Ghezelbash R, Arabkoohsar A, Pilevari L, Machado L. Employing geothermal heat exchanger in natural gas pressure drop station in order to decrease fuel consumption. Energy 2015;83:164–76.
[17] Arabkoohsar A, Farzaneh-gord M, Deymi-dashtebayaz M, Machado L. A new design for natural gas pressure reduction points by employing a turbo expander and a solar heating set. Renew Energy 2015;81:239–50.
[18] Lo Cascio E, Ma Z, Schenone C. Performance assessment of novel natural gas pressure reduction station equipped with parabolic trough solar collectors. Renew Energy 2018;128:177–87.
[19] Borelli D, Devia F, Lo Cascio E, Schenone C. Energy recovery from natural gas pressure reduction stations: integration with low temperature heat sources. Energy Convers Manage 2018;159:274–83.
[20] Lo Cascio E, Borelli D, Devia F, Schenone C. Future distributed generation: An operational multi-objective optimization model for integrated small scale urban electrical, thermal and gas grids. Energy Convers Manage 2017;143:348–59.
[21] Botsford C, Szczepanek A. Fast charging vs. slow charging: pros and cons for the new age of electric vehicles. EVS24 International Battery, Hybrid and Fuel Cell Electric Vehicle Symposium; 2019.
[22] Luo X, Wang J, Dooner M, Clarke J. Overview of current development in electrical energy storage technologies and the application potential in power system operation. Appl Energy 2015;137:511–36.
[23] Ríos-Mercado RZ, Borraz-Sánchez C. Optimization problems in natural gas transportation systems: A state-of-the-art review. Appl Energy 2015;147:536–55.
[24] Alavi F, Lee EP, van de Wouw N, De Schutter B, Lukszo Z. Fuel cell cars in a microgrid for synergies between hydrogen and electricity networks. Appl Energy 2017;192:296–304.
[25] Luo L, Zhou S, Huang H, Gao S, Han J, Dou X. Optimal planning of electric vehicle charging stations comprising multi-types of charging facilities. Appl Energy 2018;226:1087–99.
[26] Kristoffersen TK, Capion K, Meibom P. Optimal charging of electric drive vehicles in a market environment. Appl Energy 2011;88:1940–8.
[27] Ente Italiano di Normazione, UNI9165. http://store.uni.com/catalogo/index.php/uni-9165-2004.html; 2004 [accessed 21.03.18] (in Italian).
[28] Redelivery points - SNAM. http://www.snamretegas.it/en/services/New_Delivery_Redelivery_Points/ [accessed 21.03.18].
[29] La rete di distribuzione gas a Bolzano, https://www.seab.bz.it/it/venditori-gas/la-rete-di-distribuzione-gas-a-bolzano [accessed 21.03.18] (in Italian).
[30] Caratteristiche degli impianti, http://www.entar.it/Caratteristiche-degli-impianti.htm [accessed 21.03.18] (in Italian).
[31] Descrizione impianto di distribuzione, http://www.amgasbari.it/Default.aspx?Id=175 [accessed 21.03.18] (in Italian).
[32] Camacho EF, Bordons Alba C. Model predictive control. Springer Science & Business Media; 2013.
[33] Ternoveanu A, Ngendakumana P. Dynamic model of a hot water boiler. In: Proceedings of the climate 2000 conference, Brussels, Belgium; 1997.
[34] Geankoplis CJ. Transport processes and separation process principles: (includes unit operations). Prentice Hall Professional Technical Reference; 2003.
[35] Duffie JA, Beckman WA. Thermal processes solar engineering. 4th ed. Wiley; 2013.
[36] Jean-Jacques B, Bruno D, François M. Modelling of a pressure regulator. Int J Press Vessels Pip 2007;84:234–43.
[37] Ernst G, Keil B, Wirhser H, Jaeschke M. Flow-calorimetric results for the massic heat capacity cP and the Joule-Thomson coefficient of CH4, of (0.85 CH4 + 0.15 C2H6), and of a mixture similar to natural gas. J Chem Thermodyn 2001;33:601–13.
[38] Osiadacz AJ, Chaczykowski M. Comparison of isothermal and non-isothermal pipeline gas flow models. Chem Eng J 2001;81:41–51.
[39] Krichel SV, Sawodny O. Non-linear friction modelling and simulation of long pneumatic transmission lines. Math Comput Modell Dyn Syst 2014;20:23–44.
[40] Coelho PM, Pinho C. Considerations about equations for steady state flow in natural gas pipelines. J Braz Soc Mech Sci Eng 2007;29:262–73.
[41] Matworks. https://it.mathworks.com/help/simulink/sfg/writing-level-2-matlab-s-functions.html [accessed 01.05.18].